A Digital Glacier Database for Svalbard

Max König[1], Christopher Nuth[2], Jack Kohler[1], Geir Moholdt[2] and Rickard Pettersen[3]

[1]Norwegian Polar Institute, Fram Center, N-9296 Tromsø, Norway

[2]Dept. of Geosciences, University of Oslo, P.O.Box 1047 Blindern, 0316 Oslo Norway

[3]Dept. Of Earth Sciences, University of Uppsala, S-752 36 Uppsala

Abstract

The archipelago of Svalbard presently contains approximately 33,200 km^2 of glaciers, with a large number of small valley glaciers as well as large areas of contiguous ice fields and ice caps. While a first glacier inventory was compiled in 1993, there has not been a readily available digital version. Here we present a new digital glacier database, which will be available through the GLIMS project. Glacier outlines have been created for the years 1936, 1966-71, 1990, and 2001-2010. For most glaciers, outlines are available from more than one of these years. A complete coverage of Svalbard is available for the 2001-2010 dataset. Glacier outlines were created using cartographic data from the original Norwegian Polar Institute topographic map series of Svalbard as basis by delineating individual glaciers and ice streams, assigning unique identification codes relating to the hydrological watersheds, digitizing center-lines, and providing a number of attributes for each glacier mask. The 2001-2010 glacier outlines are derived from orthorectified satellite images acquired from the SPOT-5 and ASTER satellite sensors. In areas where coverage for all time periods is available, the overwhelming majority of glaciers are observed to be in sustained retreat over the period from 1936-2010.

Introduction

Approximately 60% of Svalbard is covered by glaciers, including valley glaciers, ice fields and the large ice caps on Nordaustlandet. The first complete glacier inventory of Svalbard was presented by Hagen et al. (1993; herein referred to as H93), following the instructions of the World Glacier Inventory. The H93 inventory was based upon the original topographic map series of Svalbard derived from aerial photographs taken over multiple years (1936/1966/1971). Attributes such as area and length were directly measured from these maps and documented in tables. The original data (i.e. glacier masks) are not available in any digital format, although the original hard-copy atlas can be found as an electronic publication (http://brage.bibsys.no/npolar/).

Today, mapping data can be stored digitally, and geographic information systems (GIS) provide a platform from which to organize geographic data and associated attributes. The objectives of this work is to convert and enhance the original H93 Svalbard glacier atlas into digital format, where individual years of each glacier mask can be obtained along with digital records of the location of these masks and glacier front positions. Additionally, a new compilation of glacier masks from recent

satellite images is created, to provide the most up-to-date glacier inventory of the Svalbard archipelago.

Regional Context

Svalbard is a high arctic archipelago located north of mainland Norway between Greenland and Novaya Zemlya at approximately 78° N 16° E (Figure 1). Svalbard's location between the Fram Strait and the Barents Sea at the outer reaches of the North Atlantic warm water current (Loeng, 1991) results in Svalbard experiencing a relatively warm and variable climate as compared to other regions at the same latitude. The winter sea ice cover of the Arctic Ocean to the North limits moisture supply while in the region South of Svalbard cyclones gain strength as storms move northward (Tsukernik et al., 2007). These geographical and meteorological conditions make the climate of Svalbard not only extremely variable (spatially and temporally), but also sensitive to deviations in both the heat transport from the south and the sea ice conditions to the north (Isaksson et al., 2005).

The Svalbard archipelago comprises four major islands with a total area of ~61,000 km^2, of which roughly 60% is covered by glaciers (Hagen et al., 1993). Glacier types include valley glaciers, ice fields and ice caps. Svalbard glaciers are generally polythermal (Björnsson et al., 1996; Hamran et al., 1996; Jania et al., 2005; Palli et al., 2003), and many of them are surge type (Hamilton and Dowdeswell, 1996; Jiskoot et al., 2000; Murray et al., 2003b; Sund et al., 2009). Of the ~1,100 glaciers on Svalbard that are larger than 1 km^2, less than 20% of these terminate in tidewater, while the remainder terminate on land. Typical Svalbard glaciers are characterized by low velocities (<10 m/a) (Hagen et al., 2003b) with glacier beds often frozen to the underlying permafrost (Björnsson et al., 1996). Glacier fronts have been retreating the last 80-90 years and mass balance has been overall negative (Hagen et al. 2003b). Comparison of maps and digital elevation models (DEM) shows that there has been an accelerating rate of mass loss in recent years for western Svalbard (Kohler et al. 2007).

The largest island, Spitsbergen (37,500 km^2), is dominated by steep mountains surrounded by low flat terrain around the coastline containing ~22,000 km^2 of glaciers. To the north lies the island of Nordaustlandet (14,500 km^2), which has the two largest ice masses in Svalbard, Austfonna (8000 km2) and Vestfonna (2450km^2). To the southeast lie two smaller islands, Barentsøya (1,300 km^2) and Edgeøya (5100 km^2), which are are dominated by plateau-type terrain (Hisdal, 1985) and contain 2800 km2 of mainly smaller ice caps at lower elevations. A number of smaller islands lie off the east coast of Svalbard, some containing smaller ice masses. The most significant of these is Kvitøya, which is nearly completely covered with ice. Climate conditions are spatially variable; the relatively continental central region (Humlum,2002; Winther et al., 1998) receives 40% less precipitation than the east and south while the north experiences about half the accumulation of the south (Sand et al., 2003). More details on Svalbard glaciers can be found in Hagen et al. (2003a).

Database structure

Generating a new digital glacier inventory of Svalbard requires maintaining the original H93 glacier atlas identification codes. The original codes comprised a 5-digit system where the first 2 digits represent the regional drainage basin, the 3rd digit represents the sub-regional drainage basin, and

the last two digits indicate the specific glacier. In many cases, these codes referred to more than one glacier, which can be potentially divided into two or more glaciers based upon the locations of medial moraines. In addition, many glaciers containing single identification codes have divided into two or more individual glacier units through the ongoing frontal retreat in Svalbard. To account for this, we introduce a decimal into the original glacier codes. This maintains the original system while allowing for future progression and changes of the glaciers. The decimal also allows us to account for glaciers and snow patches smaller than 1 km^2, which will receive the same identification code that ends with "99" but with an increasing decimal for each individual small glacier or snow patch (i.e. XXX99.01, XXX99.02).

Since the original glacier atlas data are not digital, and due to the multiple year compilation of that database, this task requires re-compiling all glacier masks. All map data from the Norwegian Polar Institute was digitalized in the 1990s, which forms the basis for this glacier inventory re-compilation. Many glaciers in Svalbard are valley-type, which are easily divisible into glacier masks. However, most of the glacier area comprises connected ice fields that drain into separate valleys. To divide these into individual glacier units we follow the principle of hydrological drainage divides based upon surface topography. We use a compilation of older and newer contour lines and Digital Elevation Models as well as satellite images to help interpret the border between individual glacier units. The hydrological approach based upon topography does not account for ice flow, e.g. ice may flow in a different direction than what the surface topography suggests and the ice divide may not always coincide with the topographic divide. While these masks and divides are derived with the best possible data at the present time, we acknowledge that errors and mistakes may occur, and therefore hope to create a transparent database where mistakes, if found, can be adjusted and corrected as further information is acquired.

It is important to note that the glacier inventory presented in this paper follows the original H93 glacier atlas, using the same definition of individual glaciers, drainage basins and identification codes. The Global Land Ice Measurements from Space (GLIMS) project follows a somewhat different definition of glaciers and identification codes (Raup and Khalsa, 2010). Within GLIMS, for example, glaciers sharing one and the same terminus are defined as one glacier unit, whereas in H93 individual ice streams may be defined as separate glaciers even though sharing the same terminus. The glacier inventory presented in this paper will eventually be available in two versions, one available through the Norwegian Polar Institute following the H93 glacier definition and another one available through the GLIMS website following the GLIMS specifications as described in Raup and Khalsa (2010).

Data

The original Topographic Map Series of Svalbard (S100) – 1936 / 1966 / 1971

The Norwegian Polar Institute (NPI) has created photogrammetric topographic maps for Svalbard since the 1930s (Luncke, 1949). The original S100 Topographic Map Series of Svalbard is based on aerial photography and surveys taken during campaigns in 1936, 1938, 1960, 1966, and 1969-71. The first campaigns in 1936 and 1938 acquired oblique aerial photography from 2500-3000 m a.s.l. while the later campaigns acquired vertical aerial photography. The map series was created at 1: 100 000

scale and with 50 meter contour interval. The accuracy and precision of the 1936/38 maps is limited due to the technology available at the time and to the relatively high flight altitudes. The uncertainty of glacier contours varies by elevation, with upper elevation contours less accurate than those at lower elevations due to the lower image contrast in the accumulation areas. In addition, the flight plan for the early aerial photography campaigns was preferentially flown around the coast looking inland, such that the distance to the image point of the higher-elevation areas was typically greater than that for lower elevation points (Nuth et al., 2007). The horizontal accuracy of the 1936/38 data can be 20-50 m, or even worse in some places. Topographic maps from 1960-1971 were created from vertical aerial photography obtained in late summer, which were analyzed using analog stereographic equipment to yield maps at a scale of 1 : 30 000 to 1 : 50 000. The horizontal uncertainty for the 1960-71 data is estimated to be 20-30 m (Harald Faste Aas, personal communication). The vertical uncertainty of the contours is found to be around 15-20 m compared to ICESat (Nuth et. al., 2010).

The S100 topographic map series of Svalbard is thus a compilation of data from multiple years. The 1936 dataset covers about 25% of the archipelago, mainly southern and western Spitsbergen. The 1960-1971 data covers northern Spitsbergen and the eastern islands of Barentsøya and Edgeøya, about 50% of the entire archipelago. Data on Nordaustlandet were not collected until 1983 when a collaboration between The Scott Polar Research Institute (SPRI) and NPI acquired surface and bed elevations of the ice cap through radar echo sounding and pressure based altimetry (Dowdeswell et al., 1986). All archived map data were digitized in the 1990s, such that elevation contours, glacier outlines and coast lines became digitally available as shape files. The glacier outlines were, however, not divided into individual glaciers, but they only delineated connecting ice masses. Therefore considerable analysis is required to convert the original, cartographic shapefile into a useable glacier database.

The 1990 photogrammetric survey

The 1990 campaign acquired vertical aerial images in late summer from a height of ca. 8000 m-a.s.l. The entire archipelago was covered, except for two swaths along the central ridge of the south eastern coast. The 1990 maps represent an improvement over the previous S100 maps in that the newer maps were made using digital photogrammetric techniques; automated image matching replaced the analogue stereoscopic plotter, and map quality became less dependent on the skill of the photogrammetrist.

DEMs and orthophotos have been created from the 1990 images for approximately 30% of the archipelago after the photogrammetric survey. The basic NPI S100 database has been updated with these 1990 map products. However, the completion of the 1990 map products has officially been abandoned for a new generation of DEMs acquired from an ongoing aerial photogrammetric campaign started in 2007. The 1990 DEMs typically have a ground resolution of 20 m and a horizontal and vertical uncertainty of less than ±5 m (Nuth et al., 2007; Nuth et al., 2010).

The Satellite dataset

The main basis for the satellite-based glacier database is the IPY SPIRIT (SPOT 5 stereoscopic survey of Polar Ice: Reference Images and Topographies) project (Korona et al., 2009) which provided high resolution DEMs (40m/pixel) and orthophotos (5m/pixel) covering approximately 70% of the

archipelago (Figure 2). The High Resolution Stereoscopic (HRS) Sensor onboard SPOT 5 contains 2 telescopes looking forward and backward 20° from nadir. The DEMs are automatically generated and geolocated with horizontal precisions better than 30 m (Bouillon et al., 2006; Nuth and Kääb, 2011, Nuth et al., in press). Vertical uncertainty is within ±10 m (Korona et al., 2009), although in practice it is often better than 5-8 m in Svalbard under optimal light conditions (high zenith angle) during acquisitions, for increasing contrast on the white glacier surfaces). To generate a complete satellite inventory, the missing areas from the IPY SPIRIT Project are covered using automatically generated ASTER DEMs and orthophotos from 2000-present (AST14DMO product from LPDAAC). The ASTER nadir- and back-looking cameras provide a base-to-height ratio of 0.6, and automatically generated DEMs have a horizontal uncertainty sometimes up to 3 pixels (90 m) and a vertical uncertainty of 15-20 m (Nuth and Kääb, 2011). All satellite datasets are first co-registered to the higher accuracy aerophotogrammetric products following Nuth and Kääb (2011), in which the horizontal correction parameters derived for the DEMs are applied directly to the orthophotos. The resulting horizontal geo-location is then as precise as ±10 m.

Methodology

Creating glacier outlines from cartographic data for the 1936/66/71 data set

To initiate the transfer of individual glacier identification codes from H93 to digital media, we begin with the earliest cartographic shapefiles from the S100 map series (Figure 2a). Each individual glacier was separated from the original conglomerate polygon, and new metadata such as glacier name and ID added as an attribute. For individual valley glaciers not connected to a larger ice mass, the original polygon often needed minor adjustments, mainly accomplished by removing snow fields connected to the glacier surface that were originally included in the shapefile by the non-glaciologist cartographer. This was accomplished through visual inspection of orthorectified SPOT, ASTER and georectified Landsat images, and also using hillshades of the DEMs, where the mountain sides can be easily visualized.

The larger interconnected ice masses also needed to be sub-divided into individual glaciers and ice streams. We follow the drainage basin divides as in H93, making only slight adjustments where our objective interpretations differ. Ice divides are manually digitized mainly using contours lines from the more recent DEMs (1990-present). As stated above, this hydrological approach for drainage basin division assumes ice flow in the direction of the surface slope. If actual ice flow diverges significantly from the apparent surface slope in the area of the basin drainage divides, this might lead to errors. In addition, determining individual glacier basins in the oldest dataset using more recent data can introduce errors. Nonetheless, the greatest apparent changes in Svalbard glaciers are occurring at the fronts, rather than at basin divides. A subset of the glacier database for the Kongsfjorden area can be seen in Figure 3, showing among others the 1936 outlines.

Creating Outlines from cartographic data for the 1990 data set

Most of the 1990 data cover glaciers where outlines for 1936-1971 are available as well (Figure 2b). Polygons of individual valley glaciers required little adjustment from the original 1990 cartographic data and were again taken entirely from the original data except for the removal of adjacent snow fields where necessary. For the larger interconnected ice masses, ice divides were not re-analyzed

but rather copied from the previous (1936/66/71) glacier outlines. The glacier identification codes were simply transferred from the older (S100) dataset to the 1990 dataset, where applicable. This method assumes that the accumulation area divides between ice masses have not changed significantly over the years. Again, most area changes of individual glaciers and ice streams occurs at the tongue of the glacier. Figure 3 shows frontal changes and outlines for 1990 in the Kongsfjorden area.

Creating Outlines from satellite data for the 2001-2010 data set

The satellite-derived glacier inventory dataset represents at present the only complete areal coverage of Svalbard derived within a short time span (Figure 2c). For this dataset, we update front positions (retreat or advance) by clipping or extending glacier outlines from the most recent mask (depending on availability in either the S100 or 1990 inventory). For glaciers experiencing large retreat, which is the case for most glaciers on Svalbard, the valley sides were also updated because there has also been concurrent areal shrinkage. The result for this in the Kongsfjorden area is again seen in Figure 3. In addition, some glaciers tagged with a single identification code in H93 have retreated into two or more separate glacier units. For these cases, the original 5 digit glacier identification codes are retained, but updated with a decimal digit to identify the new individual units. This will have an effect on the quantification of the number of glaciers in Svalbard.

Glacier and snow patches smaller than 1 km^2

The original inventory H93 did not specifically include glaciers smaller than 1 km^2, although it did attempt to estimate the number and combined area of such units. Our new digital glacier inventory attempts to include all individual glaciers smaller than 1 km^2. However, at present they do not have an individual 5 digit identification code, but rather a single unique identification code based upon the regional drainage basin (typically XXX99) followed by a unique decimal identifier. This was done both to maintain the original structure of the glacier inventory, as well as to include an estimate on the number and size of ice/snow patches less than 1km^2. Uncertainty prevails in the determination of whether small features are indeed glaciers or rather a non-dynamic snow field; this decision is subjective and difficult to automate. Each unit in the glacier database is manually classified on a case-by-case basis using the plethora of satellite images (SPOT, ASTER and Landsat) as well as the original photographs from the aerial surveys to determine whether small snow fields indeed are a glacier.

Results

Early versions of the Svalbard glacier inventory have been used to study changes in glacier geometry and glacier elevation (Nuth et al., 2007). While a more complete analysis awaits completion of the final glacier inventory, the following is a preliminary analysis showing the potential of the new data set.

Currently, there are over 1,100 glaciers in Svalbard larger than 1 km^2, with the majority in the size class 10-30 km^2 (Figure 4). Glaciers or snow patches smaller than 1 km^2 comprise less than 1% of the total glaciated area. In combination with a digital elevation model (DEM), the glacier outlines can be used to determine glacier hypsometry, i.e. the glacier area size as a function of elevation. Glacier

hypsometry varies considerably around the archipelago (Figure 5), and depends on the underlying terrain. Region 3 and especially Region 4 are areas of higher topography, where glaciers reach elevations above 1000 m.a.s.l.

The database and hypsometries can be used to make a rough estimate of equilibrium line altitudes for all of Svalbard. The accumulation-area ratio (AAR) is an easily-measured parameter strongly related to the long-term mass balance. Typical AAR values for glaciers in balance range from 0.4 – 0.8 (Bahr et al., 2009). Using the glacier hypsometry and assuming a uniform accumulation area ratio (AAR) of 0.6 (e.g. Moholdt et al., 2010), the equilibrium line altitude (ELA) can thus be found by choosing the elevation band delineating the upper 60% of the total area, the accumulation area. Figure 6 shows that ELAs calculated in this way are located at higher altitudes in the northern and central part of Spitsbergen, consistent with the lower precipitation amounts in that area (Hagen et al., 1993).

Of course, Svalbard glaciers are not in balance, and AARs do vary even for glaciers in balance (Bahr et al., 2009), so that assuming a uniform value of AAR = 0.6 is likely inappropriate for some glaciers or areas. Indeed, long-term mass balance measurements made on four glaciers in the area of Ny-Ålesund (Kohler, unpublished) show AAR ranging from 0.2 to 0.4. However, these glaciers in western Svalbard are in an area with significantly negative mass balance (Nuth et al., 2010). Applying a "standard" choice of AAR = 0.6 is appropriate for the entire archipelago, as a rough approximation; while ELA values so determined will vary with the AAR value used, the relative spatial distribution of ELAs is insensitive to AAR choice. With the caveats raised here, the geographic pattern of widely variable ELAs shown in Figure 6 is consistent with climatic differences across the island described in the Regional Context section.

In southern Spitsbergen, we have nearly complete mapping coverage for 1936, 1990, and 2008 (Figure 2), allowing us to calculate area change for the two periods 1936-1990 and 1990-2008. Figure 7 shows the area change expressed in percent change per year. The largest area changes occur for smaller glaciers in the first period. In the second period, there is an increase in the area lost for the low-altitude glaciers to the south. An increase in the rate of mass loss in western Svalbard has previously been inferred from DEMs and other elevation data (Kohler et al., 2007) and has been attributed to the concurrent long-term increase in summer temperature (Nordlie and Kohler, 2004) observed since the 1930s. Some glaciers in Figure 7 are seen to have had an increase in glacier area (blue colors); these glaciers underwent a surge between the times of two map pairs.

Most glaciers—whether tidewater or land-terminating, large or small, debris-covered or comparatively clean ice types—have undergone retreat over both time periods detailed in Figure 7. This widespread and dominant retreat, occurring for such a wide range of glacier types and sizes, is in accordance with the observed climate change (Nordlie and Kohler, 2004). For the region shown in Figure 7, the total area retreat during the first period, last period, and the sum of both periods is, respectively, 832.5, 243.1, and 1075.6 km^2, which compares to 4,961.6 km^2 total glacier area, as of 2008.

Conclusions and Future Perspectives

The new digital inventory of Svalbard glaciers presented above contains data from multiple years, including 1936, 1938, 1960, 1966, 1969-71, 1990 and 2001-2010. The inventory derived from the

latter, 21st century satellite dataset is at present the only period for which there is a spatially complete glacier inventory of Svalbard. The inventory comprises glacier outlines in the form of shapefiles and an associated attribute table describing each individual glacier. We envision a "living inventory" (dynamic inventory), which can be updated and expanded with additional glaciological data. A more complete database for example, will include glacier centerlines and lengths, glacier hypsometries, ELA and firn line estimates, thickness measurements and volume estimates as these become available. Official publication of the dataset will occur first through a digital portal operated by the Norwegian Polar Institute, and will also be sent into the GLIMS archives at the National Snow and Ice data Center (NSIDC). In addition, the dataset will be available through the CryoClim data portal. We envision a working database where publications on Svalbard glaciers can also be linked to the database through the unique glacier identification codes and therefore the database can function as a simple reference index for Svalbard glaciers.

Acknowledgements

We would like to thank Harald Faste Aas, Roger Willy Olaussen and Anders Skoglund for providing the topographic data and for advice regarding this data. Also, Boele Kuipers for advice on GIS matters. The ASTER orthorectified images and SilcAst DEMs were provided within the framework of the Global Land Ice Measurements from Space project (GLIMS) through the USGS LPDAAC and is courtesy of NASA/GSFC/METI/ERSDAC/JAROS and the US/Japan ASTER science team. The SPOT5-HRS orthorectified images and DEM were obtained through the IPY-SPIRIT project (Korona et al., 2009)© CNES 2008 and SPOT Image 2008 all rights reserved. This work is a contribution to the ESA Climate Change Initiative Project "Glaciers CCI" (Essential Climate Variable CCI ECV glaciers and ice caps). This work is in part funded by the Norwegian Space Centre as part of ESA's PRODEX program through the CryoClim project.

Figure 1: The Svalbard archipelago

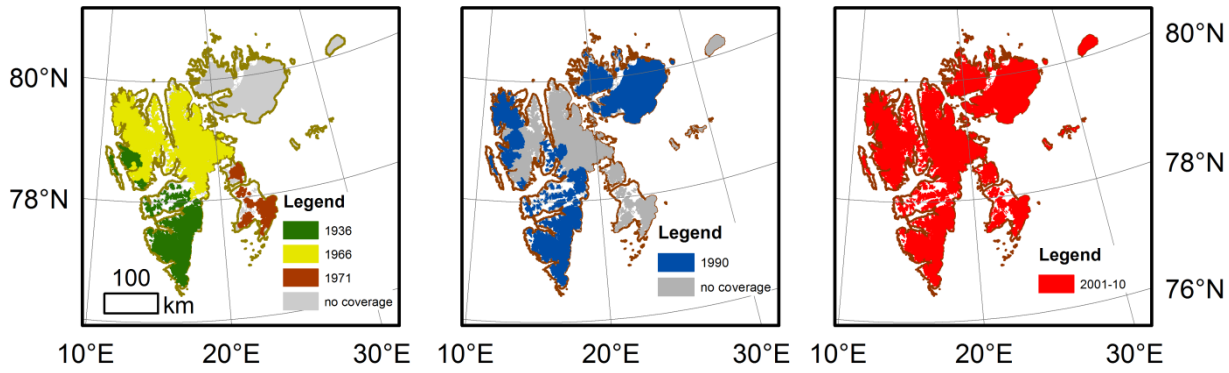

Figure 2a-c: Svalbard maps showing coverage of the three temporal datasets with glacier outlines derived from cartographic data (1936-1990) and SPOT images (2001-2010; ©CNES 2008)

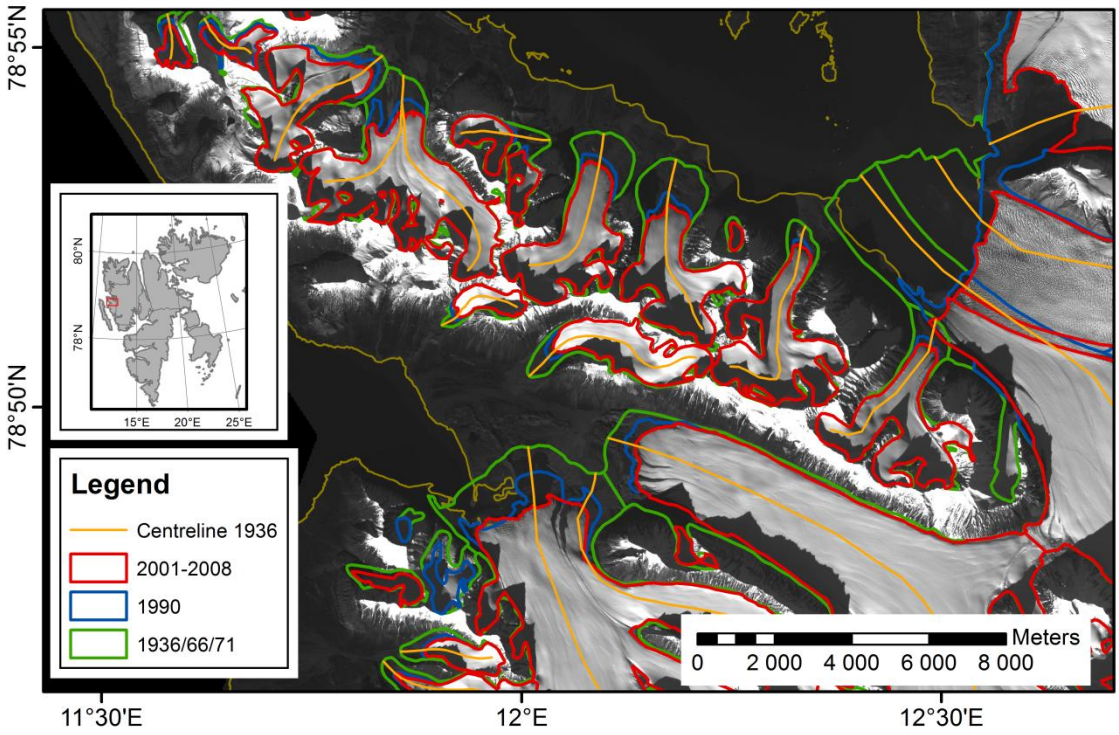

Figure 3: A subset of the database shows all available data at Brøggerhalvøya with a 2007 SPOT image (CNES 2008) as background. The colours of the glacier outlines correspond to the colours indicating data collection years in Figure 2. Retreat of the glaciers between 1936 and 2007 is clearly evident with a decrease of 3% glaciated area in Kongsfjorden. Centerlines for each glacier are also shown. We note that the glacier tongue to the far right is divided into individual tributaries following the glacier inventory by Hagen et al. (1993). GLIMS would consider these tributaries being part of a single glacier.

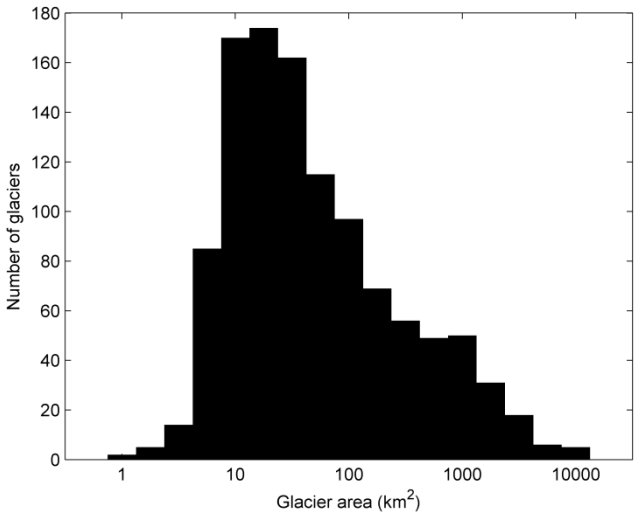

Figure 4: Distribution of glaciers sizes for Svalbard. There are over 1,100 glaciers in Svalbard larger than 1 km^2, with the majority in the size class 10-30 km^2. Glaciers or snow patches smaller than 1 km^2 comprise less than 1% of the total glaciated area.

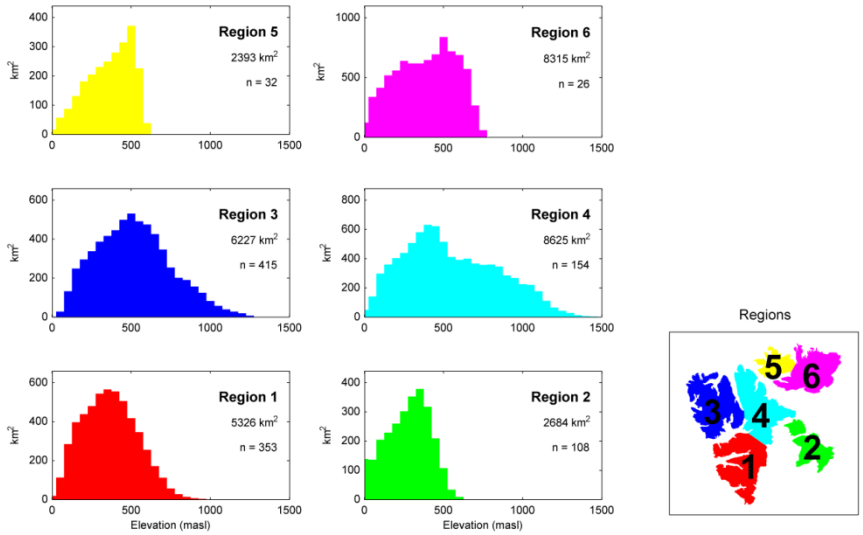

Figure 5: Glacier hypsometry for different regions on Svalbard.

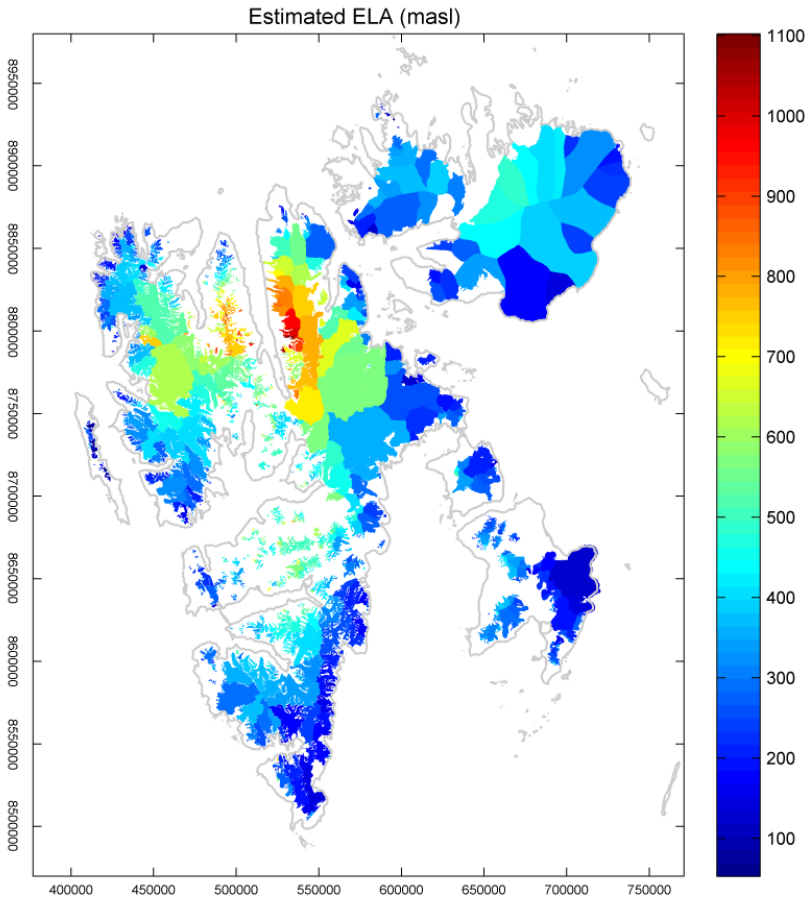

Figure 6: ELA distribution for Svalbard, estimated from individual glacier hypsometries and assuming constant AAR = 0.6. Estimated ELAs are located at higher altitudes in the northern and central part of Spitsbergen, corresponding to the lower precipitation amounts in that area (Hagen et al., 1993).

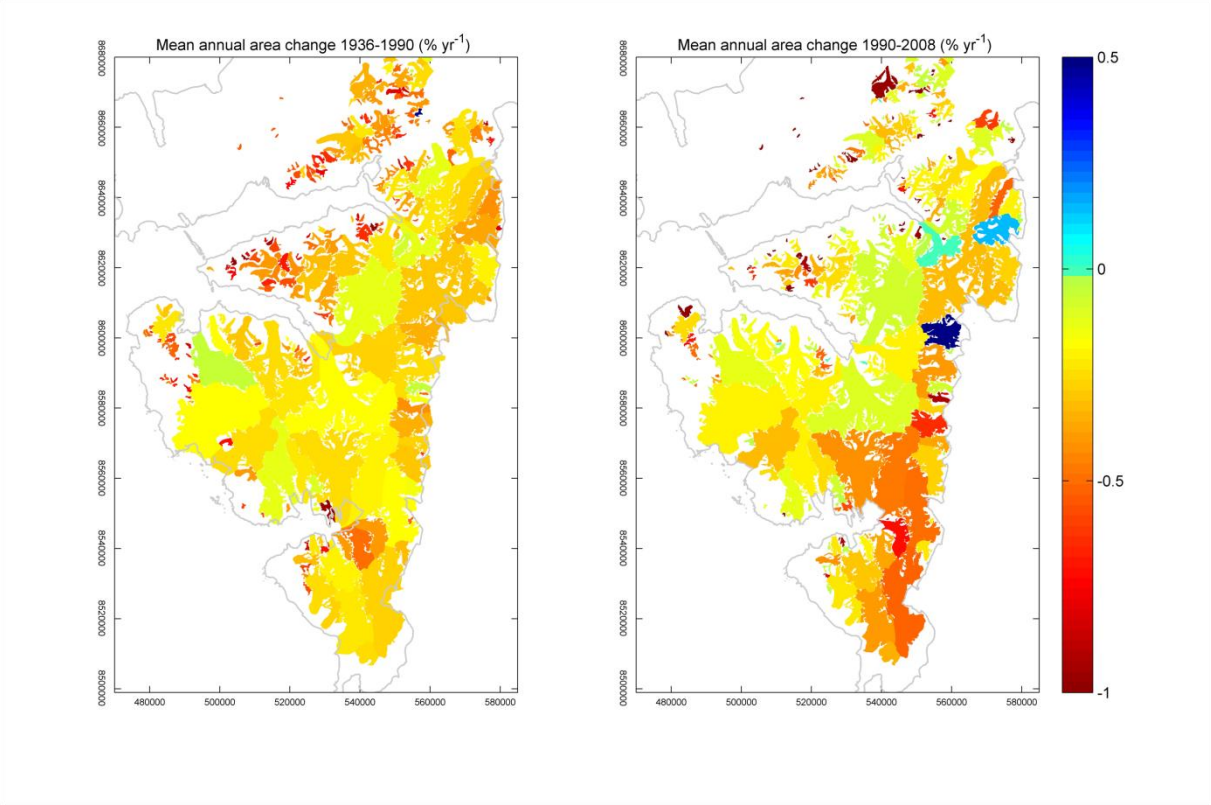

Figure 7: Annual glacier area change in percentage per year for 1936 to 1990 and 1990 to 2008, relative to 1936 and 1990, respectively. Glaciers with an increase in glacier area (blue colors) underwent a surge between the two maps.

References

Bahr, D. B., M. Dyurgerov and M. F. Meier (2009). "Sea-level rise from glaciers and ice caps: A lower bound." Geophysical Research Letters **36**.

Björnsson, H., Y. Gjessing, S. E. Hamran, J. O. Hagen, O. Liestøl, F. Palsson, and B. Erlingsson (1996). The thermal regime of sub-polar glaciers mapped by multi-frequency radio-echo sounding, Journal of Glaciology, **42**(140): 23– 32.

Blaszczyk, M., J. A. Jania and J. O. Hagen. 2009. Tidewater glaciers of Svalbard: Recent changes and estimates of calving fluxes. Polish Polar Research, Vol. 30, no. 2, pp. 85–142.

Bouillon, A., M. Bernard, P. Gigord, A. Orsoni, V. Rudowski and A. Baudoin (2006). "SPOT 5 HRS geometric performances: Using block adjustment as a key issue to improve quality of DEM generation." ISPRS Journal of Photogrammetry and Remote Sensing **60**(3): 134 - 146.

Dowdeswell, J., D. J. Dewry, A. P. R. Cooper, M. R. Gorman, O. Liestøl and O. Orheim (1986). "Digital mapping of the Nordaustlandet ice caps from airborne geophysical investigation." Annals of Glaciology **8**: 51-58.

Hagen, J. O., J. Kohler, K. Melvold and J. G. Winther (2003a). "Glaciers in Svalbard: mass balance, runoff and freshwater flux." Polar Research **22**(2): 145-159.

Hagen, J. O., K. Melvold, F. Pinglot, and J. A. Dowdeswell (2003b). On the net mass balance of the glaciers and ice caps in Svalbard, Norwegian Arctic, Arctic Antarctic and Alpine Research, **35**(2): 264 – 270.

Hagen, J. O., O. Liestøl, E. Roland and T. Jørgensen. (1993). Glacier atlas of Svalbard and Jan Mayen. Oslo.

Hamilton, G., and J. Dowdeswell (1996). Controls on glacier surging in Svalbard, Journal of Glaciology, **42**(140): 157–168.

Hamran, S. E., E. Aarholt, J. O. Hagen, and P. Mo (1996). Estimation of relative water content in a sub-polar glacier using surface-penetration radar, Journal of Glaciology, **42**(142): 533– 537.

Hisdal, V. (1985). Geography of Svalbard, Norw. Polar Inst., Oslo.

Humlum, O. (2002). Modelling late 20th-century precipitation in Nordenskiøld Land, Svalbard, by geomorphic means, Norwegian Journal of Geography, **56**(2), 96–103.

Isaksson, E., et al. (2005). Two ice-core delta O-18 records from Svalbard illustrating climate and sea-ice variability over the last 400 years, Holocene, **15**(4): 501– 509.

Jania, J., et al. (2005), Temporal changes in the radiophysical properties of a polythermal glacier in Spitsbergen, Annals of Glaciology, **42**: 125 – 134.

Jiskoot, H., T. Murray, and P. Boyle (2000). Controls on the distribution of surge-type glaciers in Svalbard,Journal of Glaciology, **46**(154): 412 – 422.

Kohler, J., T. D. James, T. Murray, C. Nuth, O. Brandt, N. E. Barrand, H. F. Aas and A. Luckman (2007). "Acceleration in thinning rate on western Svalbard glaciers." Geophysical Research Letters **34**(18): 5.

Korona, J., E. Berthier, M. Bernard, F. Rèmy and E. Thouvenot (2009). "SPIRIT. SPOT 5 stereoscopic survey of Polar Ice: Reference Images and Topographies during the fourth International Polar Year (2007-2009)." ISPRS Journal of Photogrammetry and Remote Sensing **64**(2): 204-212.

Loeng, H. (1991). Features of the physical oceanographic conditions of the Barents Sea, Polar Research, **10**(1): 5 – 18.

Luncke, B. (1949). "Norges Svalbard- og ishavs- undersøkelsers kartarbeider og anvendelsen av skrå-fotogrammer tatt fra fly." Norsk Polarinstitutt Meddelelser **68**.

Moholdt, G., J. O. Hagen, T. Eiken and T. V. Schuler (2010). "Geometric changes and mass balance of the Austfonna ice cap, Svalbard." The Cryosphere **4**: 1-14.

Murray, T., T. Strozzi, A. Luckman, H. Jiskoot, and P. Christakos (2003). Is there a single surge mechanism? Contrasts in dynamics between glacier surges in Svalbard and other regions, Journal of Geophysical Research, **108**(B5): 2237.

Nordli, Ø. and J. Kohler. 2004: The early 20th century warming. Daily observations at Grønfjorden and Longyearbyen on Spitsbergen (2nd edition). DNMI/klima report, No. 12/03.

Nuth, C., J. Kohler, H. F. Aas, O. Brandt and J. O. Hagen (2007). "Glacier geometry and elevation changes on Svalbard (1936-90): a baseline dataset." Annals of Glaciology **46**: 106-116.

Nuth, C. and A. Kääb (2011). Co-registration and bias corrections of satellite elevation data sets for quantifying glacier thickness change, The Cryosphere, 5, 271-290.

Nuth, C., G. Moholdt, J. Kohler, J. O. Hagen and A. Kääb (2010). "Svalbard glacier elevation changes and contribution to sea level rise." Journal of Geophysical Research-Earth Surface **115**.

Nuth, C., T. V. Schuler, J. Kohler, B. Altena and J. O. Hagen " Estimating the long term calving flux of Kronebreen, Svalbard, from geodetic elevation changes and mass balance modelling." Journal of Glaciology **in press**.

Palli, A., J. C. Moore, and C. Rolstad (2003). Firn-ice transition-zone features of four polythermal glaciers in Svalbard seen by groundpenetrating radar, Annals of Glaciology, **37**: 298 – 304.

Raup, B. and S. Khalsa (2010). GLIMS Analysis Tutorial, [http://www.glims.org/MapsAndDocs/assets/GLIMS_Analysis_Tutorial_a4.pdf]

Sand, K., J. G. Winther, D. Marechal, O. Bruland, and K. Melvold (2003). Regional variations of snow accumulation on Spitsbergen, Svalbard, 1997– 99, Nordic Hydrology, **34**(1– 2), 17–32.

Sund, M., T. Eiken, J. O. Hagen, and A. Kääb (2009). Svalbard surge dynamics derived from geometric changes, Annals of Glaciology, **50**, 50–60.

Tsukernik, M., D. N. Kindig, and M. C. Serreze (2007). Characteristics of winter cyclone activity in the northern North Atlantic: Insights from observations and regional modeling, Journal of Geophysical Research, 112.

Winther, J. G., O. Bruland, K. Sand, A. Killingtveit, and D. Marechal (1998). Snow accumulation distribution on Spitsbergen, Svalbard, in 1997, Polar Research, **17**(2): 155 – 164.